High resolution electron energy loss spectroscopy with two-dimensional energy and momentum mapping

Xuetao Zhu, Yanwei Cao, Shuyuan Zhang, Xun Jia, Qinlin Guo, Fang Yang, Linfan Zhu, Jiandi Zhang, E. W. Plummer, and Jiandong Guo

Citation: Review of Scientific Instruments **86**, 083902 (2015);
View online: https://doi.org/10.1063/1.4928215
View Table of Contents: http://aip.scitation.org/toc/rsi/86/8
Published by the American Institute of Physics

High resolution electron energy loss spectroscopy with two-dimensional energy and momentum mapping

Xuetao Zhu,[1,a)] Yanwei Cao,[1,a)] Shuyuan Zhang,[1] Xun Jia,[1] Qinlin Guo,[1] Fang Yang,[1] Linfan Zhu,[2] Jiandi Zhang,[3] E. W. Plummer,[3] and Jiandong Guo[1,4,b)]
[1]*Beijing National Laboratory for Condensed Matter Physics and Institute of Physics, Chinese Academy of Sciences, Beijing 100190, China*
[2]*Hefei National Laboratory for Physical Sciences at Microscale and Department of Modern Physics, University of Science and Technology of China, Hefei, Anhui 230026, China*
[3]*Department of Physics and Astronomy, Louisiana State University, Baton Rouge, Louisiana 70808, USA*
[4]*Collaborative Innovation Center of Quantum Matter, Beijing 100871, China*

(Received 14 June 2015; accepted 28 July 2015; published online 13 August 2015)

High resolution electron energy loss spectroscopy (HREELS) is a powerful technique to probe vibrational and electronic excitations at surfaces. The dispersion relation of surface excitations, i.e., energy as a function of momentum, has in the past, been obtained by measuring the energy loss at a fixed angle (momentum) and then rotating sample, monochromator, or analyzer. Here, we introduce a new strategy for HREELS, utilizing a specially designed lens system with a double-cylindrical Ibach-type monochromator combined with a commercial VG Scienta hemispherical electron energy analyzer, which can simultaneously measure the energy and momentum of the scattered electrons. The new system possesses high angular resolution (<0.1°), detecting efficiency and sampling density. The capabilities of this system are demonstrated using $Bi_2Sr_2CaCu_2O_{8+\delta}$. The time required to obtain a complete dispersion spectrum is at least one order of magnitude shorter than conventional spectrometers, with improved momentum resolution and no loss in energy resolution. © *2015 AIP Publishing LLC.* [http://dx.doi.org/10.1063/1.4928215]

I. INTRODUCTION

High resolution electron energy loss spectroscopy (HREELS) is a powerful technique to probe vibrational and electronic excitations at solid surfaces.[1] An electron with energy E_i incident on the crystal may interact with a vibrational or electronic excitation with energy $\hbar\omega$ before being backscattered. Thus, analysis of the energy of the scattered electrons, $E_s = E_i - \hbar\omega$, provides direct information of the excitations on surface or the molecules adsorbed on surface. More importantly, by analyzing the momentum along the in-plane direction, it is possible to probe the excitations throughout the entire Brillouin zone (BZ) on a single crystal surface and thus obtains the dispersion, i.e., energy as a function of momentum. HREELS has proven to be one of the most powerful methods to obtain the dispersion of phonons[2,3] and plasmons [4] on surfaces.

Dispersion measurements in a conventional HREELS system require the change of the scattering geometry by mechanically rotating sample, monochromator, or analyzer. The analyzer collects the scattered electrons at a certain angle, which carries important momentum information of vibrational and electronic excitations. The slit width of the analyzer is one of the key parameters related to the energy and momentum resolution. This is a point-by-point measurement of the energy loss spectrum for each momentum, i.e., a one dimensional (1D) detection system. The sampling density in momentum space and the according measuring reproducibility are restricted by the mechanical rotation, and the detecting efficiency is quite low. It usually takes tens of hours for the measurements to probe one direction of the BZ with a reasonable sampling density in momentum space. This long measurement time causes potential problems. Even in ultra-high vacuum (UHV), the sample surface will be contaminated after a long measurement time, which makes it difficult to identify the desired intrinsic properties. This time constraint becomes more important when HREELS is used to study multi-component complex materials, which are cleaved or grown in vacuum.

In 1990s, using hemispherical electron analyzers with two-dimensional (2D) position-sensitive detectors,[5] 2D energy and momentum mapping was realized and utilized for angle-resolved photoemission spectroscopy (ARPES) measurements. The energy of the photoelectrons is resolved in one direction according to the radii of their trajectory in the hemispherical analyzer, while their momentum is resolved in the other perpendicular direction according to their emission angle, recordable as a 2D intensity snapshot of energy versus momentum on the detector. The earliest examples of such 2D ARPES measurements are demonstrated in Refs. 6 and 7. Since then the instrument development and extensive applications have yielded tremendous advances in the understanding of electronic band structures and their renormalization related to the many-body effects in complex materials.[8–10] Considering the similar energy scale and the correspondence between electron emission/scattering angle and momentum, a new HREELS with 2D energy and momentum mapping is also

a)X. Zhu and Y. Cao contributed equally to this work.
b)jdguo@iphy.ac.cn

possible. In this work, we have developed a high-angular-resolution electron source and combined it with a hemispherical electron analyzer with multi-channel plate (MCP) detector to realize the 2D HREELS measurements. Without rotating sample, monochromator, or analyzer, a HREELS spectrum can be scanned for a certain direction through the BZ in a single measurement, and thus a momentum-dependent spectral intensity distribution can be directly obtained. Compared with conventional HREELS, the detecting efficiency and sampling density of the momentum-resolved measurements are improved by at least one order of magnitude without deteriorating the energy resolution and with an improved momentum resolution.

II. SYSTEM DESIGN

The conventional design of monochromator and analyzer used for HREELS can be traced back to 1950s to Professor Kerwin's laboratory at Laval University (Canada)[11] where a modified 127° cylindrical electron selector[12] was used in their low energy electron scattering experiments of rare gases. Based on this design, vigorous development occurred in 1960s[13–16] (with 20 meV energy resolution) which displayed the basic design of today's HREELS system. To gain high energy resolution and good signal-to-noise ratio, several later modifications were made to the lens system by Read[17] and Roy[18] in 1970s, to the cathode by Ibach in 1982 (U.S. Patent No. 4309607), to the monochromtors and lens by Kesmodel in 1985 (U.S. Patent No. 4559449), and to the analyzers and lens system by Ibach in 1989 (U.S. Patent No. 4845361). In 1990s, Ibach achieved energy resolution better than 1 meV.[19] Since that time this Ibach-type spectrometer has become the most widely used HREELS instrument, which, when combined with other techniques, produced time-resolved HREELS[20,21] and spin-polarized HREELS.[22–24] This effort in instrument development lead to many successful experiments in surface physics and surface chemistry.[4,25]

In 2000, a new type of electron energy loss spectrometer (EELS) was developed based on the spot profile analysis low-energy electron diffraction (SPA-LEED),[26] where an Ibach-type EELS monochromator was attached as an auxiliary part of the high-resolution LEED.[27] The scattered electrons from different angles were detected by the SPA-LEED, enabling momentum resolved measurements without any mechanical rotation, which would be an advantage. But this instrument could not do 2D energy-momentum mapping, since the energy loss spectra for different momenta are obtained one at a time. In addition, the energy resolution was only 18 meV.[26]

Here, we will demonstrate the use of 2D (energy-momentum) hemispherical energy analyzer, combined with an Ibach-type electron monochromator. The combination of an Ibach-type electron monochromator and hemispherical analyzer has been utilized in HREELS, studying the chemical bond vibrations in liquids.[28] It should be mentioned that, unlike the conventional Ibach-type HREELS in which the exit lens of monochromator and the entrance lens of analyzer are designed symmetric to reduce the divergence angle, the simple combination of a hemispherical analyzer with the standard cylindrical monochromator will introduce asymmetry to the electron path and severely deteriorate the angular (momentum) resolution. This may be the reason why the 2D HREELS measurements were not attempted with the system in Ref. 28. In principle the combination of a spherical monochromator and analyzer designed and used in 1960s[29–31] should be compatible with 2D detector system. But the Ibach-type double-pass electron monochromator compensating for space charge is much better than the single spherical deflector.

The angular resolution detected by a hemispherical analyzer with different electron beams from the Ibach-type monochromator can be estimated considering an ideal sample in a field free region. For a 4 eV beam with the spot size of 1 mm in diameter at the sample position, the divergence angle of the conventional Ibach-type electron source is usually larger than 1.5°, which would result in an angular resolution of about 2.2° in the hemispherical analyzer. To achieve angular resolution better than 0.3°, the divergence angle of the electron source has to be smaller than 0.1°. Thus to realize the advantages of 2D hemispherical analyzer, a new exit lens system for the Ibach-type double-pass monochromator must be designed.

A. High-momentum-resolution electron source

Figure 1 illustrates the electron optics of the new HREELS system from the electron source to the detector. The electron source is designed based on the ELS5000 double-pass electron monochromator from LK Technologies. The ELS5000, a typical Ibach-type spectrometer using a special LaB_6 cathode, employs a highly optimized double-pass monochromator whereby space charge compensation of the 127° cylindrical sector is made in both monochromator stages by careful choice of design parameters. The combination of the two monochromator provides an energy resolution to 0.5 meV under optimal conditions. The energy of the electron beam can be tuned from 1 to 200 eV. Our design is aimed at modifying the exit lens system of the ELS5000 source to improve the angular resolution while maintaining its high energy resolution.

Fig. 2 shows the details of the lens design (parts 1–3 in Fig. 1). In this arrangement, the scattering plane of the electrons is the XZ plane. The electrons scattered from the sample entering the analyzer are selected by the slit (part 14

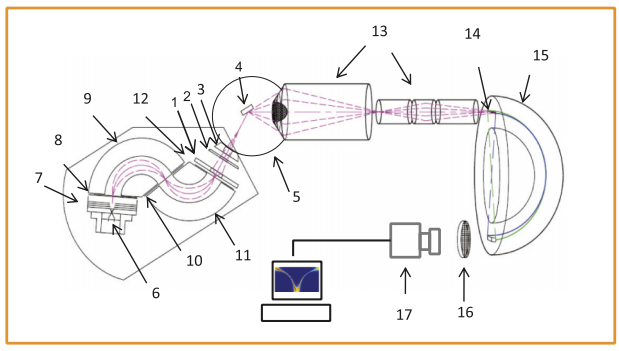

FIG. 1. Illustration of the electron optics of the HREELS system: 1-lens I, 2-lens II, 3-lens III, 4-sample, 5-equal potential shield, 6-filament, 7-repeller, 8-anode, 9-monochromator I (M1), 10-M1 aperture, 11-monochromator II (M2), 12-M2 aperture, 13-electron lenses of analyzer, 14-slit of analyzer, 15-hemispherical electron analyzer, 16-multi-channel plate, and 17-CCD camera.

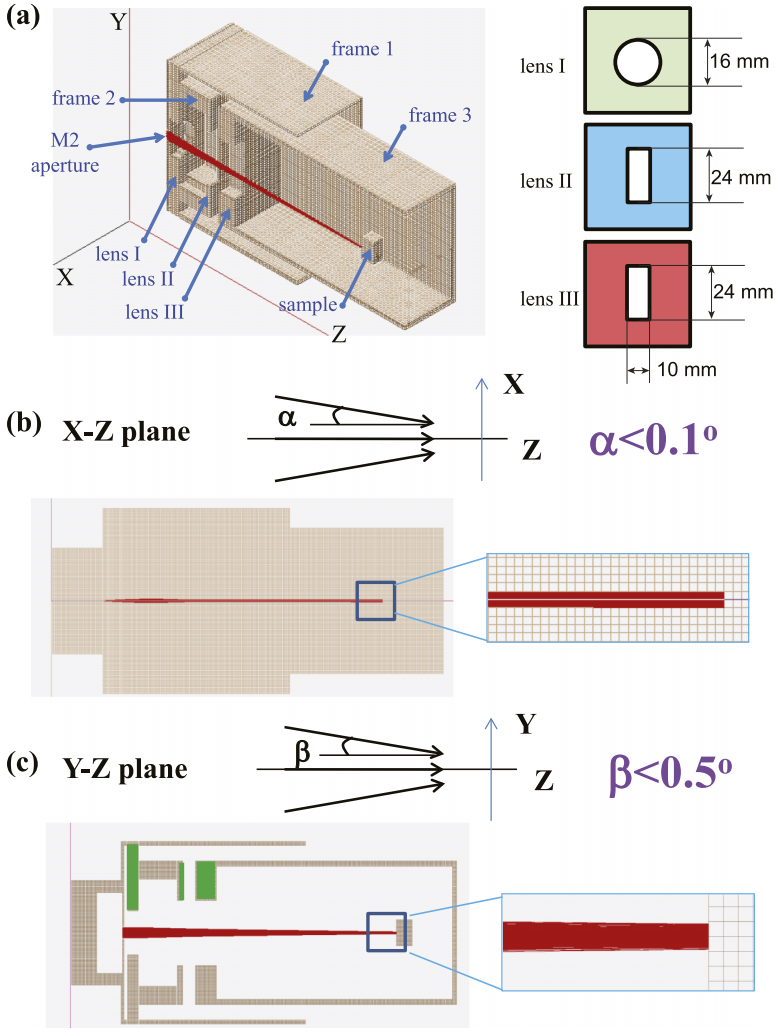

FIG. 2. Design and simulation of the exit lens system with high-angular-resolution. (a) Perspective view of the three lens elements in Fig. 1. The red line indicates the simulated trace of the electron beam. The starting position of electron beam is at the center of the M2 aperture with a rectangular shape (0.3 mm in X-Z plane and 4 mm in Y-Z plane). The angular dispersion at the starting position is [−3°, 3°] in X-Z plane whereas it is [−0.76°, 0.76°] in Y-Z plane. The beam energy is 4.3 eV and we assume the space charge is nearly 10^{-9} A. (b) Top view of panel (a) which shows the horizontal divergence angle α of the beam. The simulated value of α is less than 0.1°. (c) Front view of panel (a) which shows the vertical divergence angle β of the beam. The simulated value of β is less than 0.5°.

in Fig. 1) of the hemispherical analyzer, which is located along the X axis (not shown here). So the momentum resolved measurements are obtained through the angular distribution of the electrons along the X axis, and the energy resolution of the analyzer is mainly determined by the slit width (along the Y axis). The angular divergence of the beam is defined by two angles: α in X-Z plane and β in Y-Z plane. As a result, the value of α constrains the angular (momentum) resolution while β has a strong effect on the signal intensity for a fixed slit size. Thus to achieve high-angular-resolution electron beam, the key is optimizing the parameters of the three lenses to effectively reduce both α and β. Ibach has proposed a scheme of HREELS electron source with high-angular-resolution mode in 1991.[32] In the current work, we adopt his scheme and determine the parameters of the lens system by the simulation with SIMION software. The lens system is composed of three metal plates with different shapes of apertures at the centers [see Fig. 2(a) and parts 1–3 in Fig. 1], respectively. The electron beam at the center of the M2 aperture with a rectangular shape (0.3 mm in X-Z plane and 4 mm in Y-Z plane) and the angular divergence in X-Z/Y-Z plane of ±3°/±0.76° is adapted, which is achievable by the Ibach-type monochromator.[32] By tracing the electron trajectories through the lens system, we determine the modified angular divergence (α in X-Z plane and β in Y-Z plane) with different positions and potentials of each lens [I-III in Fig. 2(a)]. The optimized positions of lens I, II, and III are 4 mm, 22 mm, and 32 mm from the M2 aperture of the monochromator, and the applied voltages on them are −0.009 V, 0.5 V, and 4 V, respectively, which result in the minimized α/β of 0.1°/0.5°, as shown in Figs. 2(b) and 2(c).

It should be also mentioned that in sharp contrast to the lens system used in the two main commercial HREELS's (Delta0.5 from SPECS and LK5000 from LK technologies) with long distance between the first lens (part 1 in Fig. 1) and the M2 aperture (part 12 in Fig. 1), the distance in high-angular-resolution lens system is very short. Moreover, in high-angular-resolution lens system, the distance between the M2 aperture (part 12 in Fig. 1) and sample (part 4 in Fig. 1) is increased from 60 mm to 105 mm to enlarge the

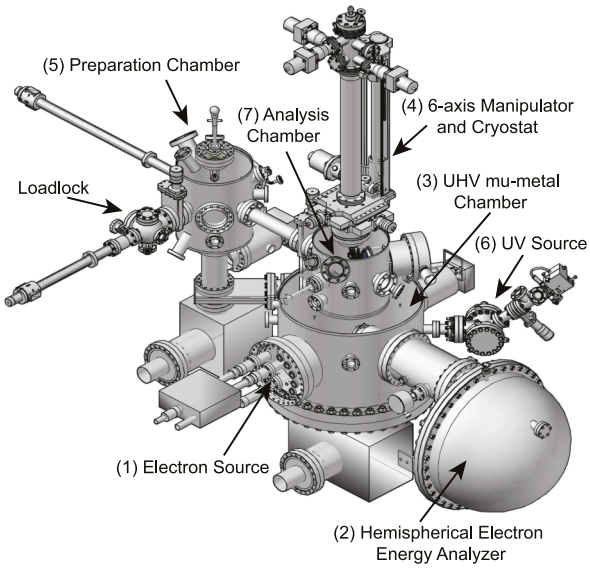

FIG. 3. Illustration of the system design. As labeled by arrows in the figure, the setup is composed of the following main parts: (1) incident electron source; (2) hemispherical electron energy analyzer; (3) UHV mu-metal measurement chamber; (4) sample manipulator and cryostat; (5) preparation chamber and sample transfer system; (6) UV light for ARPES measurement; and (7) analysis chamber. Functionally the system is an integration of HREELS and ARPES sharing the same hemispherical electron energy analyzer, but with different incident beams of monochromated electrons and UV light, respectively.

magnification of the angular dispersion to improve the angular resolution.[32] Replacing the lens system of the conventional Ibach-type monochromator LK5000 with the new design is essential to achieve high-angular-resolution electron beam and thus to realize the 2D HREELS measurements.

The constructed electron source is placed on a rotatable horizontal plate, whose rotation axis is the vertical central axis of the chamber (along the Y direction in Fig. 2). The sample polar rotation is also around this rotation axis. By adjusting the coaxial rotations of the electron source and the sample, the beam incident angle θ_i, defined by the angle between the sample normal and the incident beam, can be tuned in a range of 50°–90°. The position of the electron source in the system is labeled in Fig. 3.

B. Hemispherical electron energy analyzer

The electrons scattered from the surface are measured using a high resolution hemispherical electron analyzer, Scienta R4000 from VG Scienta (Fig. 3). This analyzer can be optimized to obtain ultra-high energy resolution that reaches the sub-meV region. For example, with the 0.1 mm wide slit and using a pass energy of 1 eV, the energy resolution of the analyzer is 0.25 meV. This is well matched to the narrow energy linewidth (0.5 meV) of our electron source, which allows for the total energy resolution of the HREELS system to reach 1 meV. The 2D detection scheme of R4000 simultaneously measures the energy of scattered electrons over a wide acceptance angle. The electron angular distribution can be chosen using one of the three angular resolving modes, 30°, 14°, and 7°, respectively. The 30° angular mode is selected to cover large momentum space in one measurement. Moreover, the wide angle lens in R4000 enables measurement of angle-resolved spectra over a wide kinetic energy range of 0.2–1000 eV. The angular dispersion and resolution are kept constant within this energy range. This is compatible with our electron source that can tune the energy of the electron beam from 1 to 200 eV.

C. Ultrahigh vacuum system with double μ-metal chamber

The outgoing angle of the scattered electrons from the sample carries important information about the momentum of the electrons. Besides UHV, it is also crucial to minimize the residual magnetic field to make sure the trajectory of the electron beam unaffected. In order to effectively screen the earth field or the magnetic field from surrounding environment, we chose to use double μ-metal shield for the measurement chamber (shown in Fig. 3). With this shielding, the remanent field in the sample region reaches a low level of 2 mG. A molecular turbo pump, an ion pump, and a titanium sublimation pump are connected to the measurement chamber to obtain UHV. After baking, the base pressure can reach a level as low as 1.0×10^{-10} Torr.

D. Sample manipulator and cryostat

The sample manipulator is a Cryoax 6 from VG Scienta (Fig. 3), which provides six axes of high precision sample motion. The linear motions are based on the Omniax translators for X, Y, and Z translations, whose accuracies of X, Y, and Z movements are 0.001, 0.001, and 0.01 mm, respectively. The sample stage is supported on a dedicated assembly that can provide three independent rotations—polar, azimuthal, and tilt, all with an angle accuracy of 0.005°. The linear Z motion and all the three rotations are driven by stepper motors (McMillan Motion Control, Inc.) providing smooth, accurate, and repeatable motions free from belt slip or temperature induced errors. The Cryoax 6 cryostat is installed into the core of the manipulator support tube and extends down through this tube to terminate in a heat exchanger anchored close to the rear of the sample stage. A short length of flexible copper braid connects the heat exchanger to the sample mounting plate. The cryostat is cooled by continuous flow of liquid helium. Two silicon diodes (LakeShore, DT-670) are connected to the heat exchanger and the sample mounting plate, respectively, to measure the temperature with an accuracy of 1 K. The lowest obtainable temperature is 9 K on the heat exchanger and 20 K on the sample mounting plate. The measured lowest sample temperature can reach 35 K. A ceramic button heater is mounted on the heat exchanger to vary the sample temperature between 35 and 350 K. The heater is controlled by a Scientific Instruments 9700 temperature controller, which can make the sample temperature stabilized within 1 K.

E. Preparation chamber and sample transfer system

An UHV preparation chamber equipped with a 5-axis manipulator, an ion-sputtering gun, several evaporation sources, a loadlock, and a wobble stick is part of the total system

(Fig. 3). The 5-axis manipulator, including X, Y, Z linear motions as well as polar and azimuthal rotations, equipped with a cryostat with liquid nitrogen syphons and a resistive heater allows for sample preparation. This arrangement allows us to cleave, sputter, grow, or anneal samples in a temperature range from below 100 K up to 1200 K. A loadlock (Fig. 3) is connected to the preparation chamber enabling the transfer of samples into and out of the chamber from air without breaking UHV in the preparation chamber. The base pressure in the preparation chamber can reach a level as low as 6.5×10^{-11} Torr. The prepared samples can be transferred by a magnetic arm to the Cryoax 6 manipulator in the analysis chamber (Fig. 3), where a LEED can be used to characterize the sample surface and determine the crystallographic direction. The analysis chamber is located right above the measurement chamber; thus, the Z motion of Cryoax 6 manipulator is used to transfer the sample down to the measurement chamber. All these sample transfers are operated in UHV.

F. UV light source for ARPES measurements

The system is equipped with the combination of VUV5000 UV-source and VUV5047 UV-monochromator from VG Scienta, which provides UV light at 21.2 eV (helium I) and 40.8 eV (helium II). The monochromator exit stage is equipped with a customized tapered exit capillary, which creates a small light spot (of the order of 0.5-0.6 mm FWHM) on the sample. With this UV light source, the system can run either in HREELS mode with an electron source or in ARPES mode with light source, as indicated in Fig. 3. The two modes can be easily switched by rotating the sample in UHV.

III. SYSTEM PERFORMANCE

A. Electron beam test

As mentioned previously, it is critical to minimize the divergence angle of the electron beam in order to obtain good resolutions with the hemispherical analyzer. Thus, the first task is to test the spacial distribution and angular divergence of the electron beam from the monochromator. A metal plate with a 0.5 mm × 10 mm slot was fabricated and attached to the sample holder anchored to the Cryoax 6 manipulator, so that the position of the slot can be precisely controlled. The electron source was set directly facing the energy analyzer, and the slot was placed vertically along the y-axis, as shown in Fig. 4(a). All the voltage parameters applied to the electrodes of the electron source, as indicated by part 1–part 12 in Fig. 1, were carefully tuned via the LK5000 software. Once the optimal set of parameters are fixed, the plate was moved along both the x and z axes, and the intensity of the transmitted electron beam was recorded as a function of x and z. Using a 50 eV electron beam, we recorded five different z positions. The line profiles along x-axis of these five positions are plotted in Fig. 4(b). The linewidths of these line profiles are obtained by Gaussian fittings. From those fittings we determine that the beam spot size at the sample position (usually set at the center of the chamber, corresponding to z ≃ 0 mm here in the plots) is smaller than 0.5 mm (FWHM). The horizontal

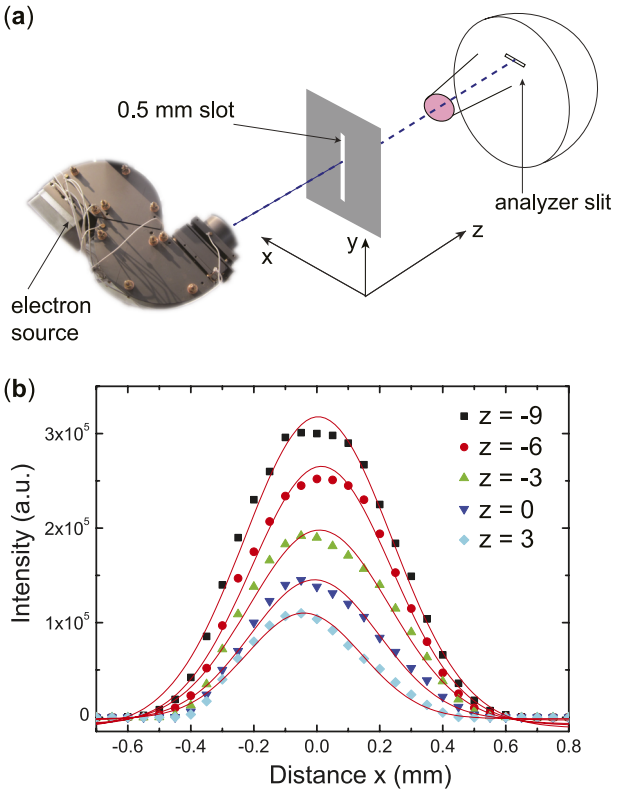

FIG. 4. Test of spacial distribution of the electron beam and the divergence angle. (a) A metal plate with a 0.5 mm wide slot was set in front of the electron source. The intensity of the electron beam through the slot was measured as a function of x and z. (b) The intensity line profiles as a function of x for five different z positions (−9, −6, −3, 0, and 3 mm) fitted by Gaussian functions.

divergence angle is calculated to be $\alpha \simeq 0.3°$, which agrees with the simulations presented in Fig. 2(b). Similar tests can be performed when the slot was placed along the x-axis and moved along both the y and z axes. This procedure provided the best set of electrode voltage parameters to generate an electron beam with the smallest divergence angle.

The highest sample current from the electron source, when the pass energies of the two monochromators are 1.54 eV and 0.8 eV, can reach 300 pA, which is comparable to the conventional Ibach-type source. If the MCP voltage of the R4000 analyzer is set to be 1400 V, 1 pA sample current is equivalent to an intensity of 5000 counts per second (CPS) in the detector of R4000.

B. Energy and momentum resolution test

The energy and momentum resolution of the system can be tested using a straight through beam with no sample as shown in Fig. 4(a) if the metal plate is removed. Fig. 5 shows the result when the incident electron energy is $E_i = 7.4$ eV, the pass energies of the two monochromators are $E_P^1 = 1.54$ eV and $E_P^2 = 0.2$ eV, respectively, the slit width of the analyzer is $w_s = 0.1$ mm, and the pass energy of the analyzer is $E_P^D = 1$ eV. The 2D detector generates an image of the beam in energy and momentum. Fig. 5(a) is such an image of the direct beam, with the horizontal axis representing the energy distribution, and the vertical axis the angle or momentum.

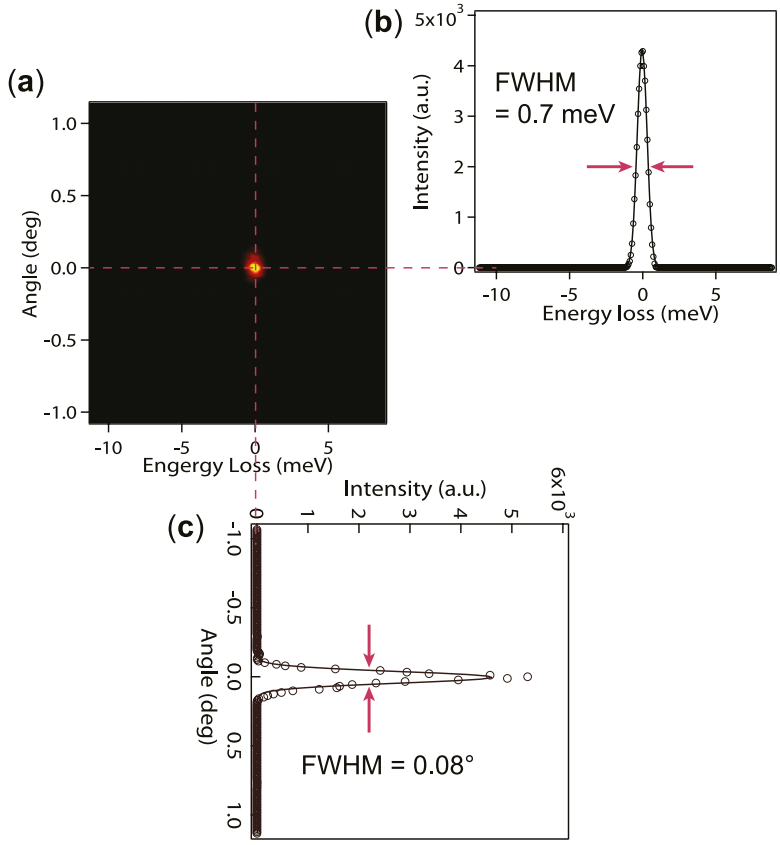

FIG. 5. Test of the energy and momentum resolution of the direct electron beam. The energy of the electron beam E_i is 7.4 eV. The pass energies of the two monochromators are 1.54 eV and 0.2 eV, respectively. The slit of the analyzer is set to be 0.1 mm and the pass energy of the analyzer is 1 eV. (a) The 2D energy-angle mapping of the direct beam. (b) The angle scale is integrated to show the intensity as a function of the energy loss, which is Gaussian fitted with FWHM = 0.7 meV. (c) The energy loss scale is integrated to show the intensity as a function of the angle, which is Gaussian fitted with FWHM = 0.08°.

The angle scale is integrated to show the intensity as a function of the energy loss in Fig. 5(b), which is Gaussian fitted with FWHM = 0.7 meV. The energy loss scale is integrated to show the intensity as a function of the angle in Fig. 5(c), which is Gaussian fitted with FWHM = 0.08°. Thus, the ultimate energy resolution for the aforementioned configuration is $\Delta E = 0.7$ meV and the angular resolution is $\Delta\theta = 0.08°$. The momentum resolution was calculated by $\Delta k = \frac{1}{\hbar}\sqrt{2m_e E_i}\cos\theta_i \Delta\theta$, where m_e is the electron mass. For a direct beam with $\theta_i = 0$ and $E_i = 7.4$ eV, we obtain the momentum resolution $\Delta k \simeq 0.002$ Å^{-1}. This Δk corresponds to about 0.3% of the BZ width for a crystal with a typical lattice constant of 4 Å. For the conventional HREELS with $\Delta\theta \simeq 1°$, $\Delta k \simeq 0.02$ Å^{-1} corresponds to 3% of the aforementioned typical BZ width.

It is important to point out that the above ultimate resolutions are obtained in optimal conditions using relatively small incident beam energy ($E_i = 7.4$ eV), smallest slit width ($w_s = 0.1$ mm) in the analyzer, lowest possible pass energies for the monochromators ($E_P^1 = 1.54$ eV/$E_P^2 = 0.2$ eV), and the analyzer ($E_P^D = 1$ eV). In a real measurement, in order to reach large momentum values, one needs to use large incident beam energies and trade-off resolutions to increase intensity by using larger slit width and pass energies. For example, if we use $E_i = 50$ eV, $w_s = 0.2$ mm, $E_P^1 = 1.54$ eV, $E_P^2 = 0.4$ eV, and $E_P^D = 2$ eV, the energy and momentum resolutions are $\Delta E \sim 3$ meV and $\Delta k \sim 0.01$ Å^{-1}, respectively.

C. Measurements on Bi2212

The overall performance of our HREELS system was tested using $Bi_2Sr_2CaCu_2O_{8+\delta}$ (Bi2212) high-Tc cuprate superconductor as the sample. Bi2212 is easy to cleave *in situ*, producing flat surface, and previous HREELS data[33] taken with a conventional spectrometer revealed dispersion in one of the optical phonon branches. In Fig. 6(a), we show the LEED pattern of Bi2212 at room temperature with the incident electron energy of 70 eV. The (1×5) surface structural reconstruction[34,35] can be clearly seen in the pattern. The HREELS measurements are performed with $E_i = 50$ eV, $\theta_i = 60°$, $w_s = 0.2$ mm, $E_P^1 = 1.54$ eV, $E_P^2 = 0.4$ eV, and $E_P^D = 5$ eV. Figs. 6(b) and 6(c) show the images on the 2D detector for directions parallel and perpendicular to the reconstruction, respectively. The excitation momentum can be determined from the scattering angles by equation

$$q = \frac{\sqrt{2m_e E_i}}{\hbar}(\sin\theta_i - \sin\theta_f), \quad (1)$$

where m_e is the static electron mass, E_i is the energy of the incident beam, θ_i and θ_f are the angles of the incident and scattered electrons, respectively. The elastic spots (zero-loss features) along the momentum axis are well-defined due to the strong intensity of the electron beam. The fractional spots due to the reconstruction along the y direction are clear in Fig. 6(b). This feature is very helpful to determine the position

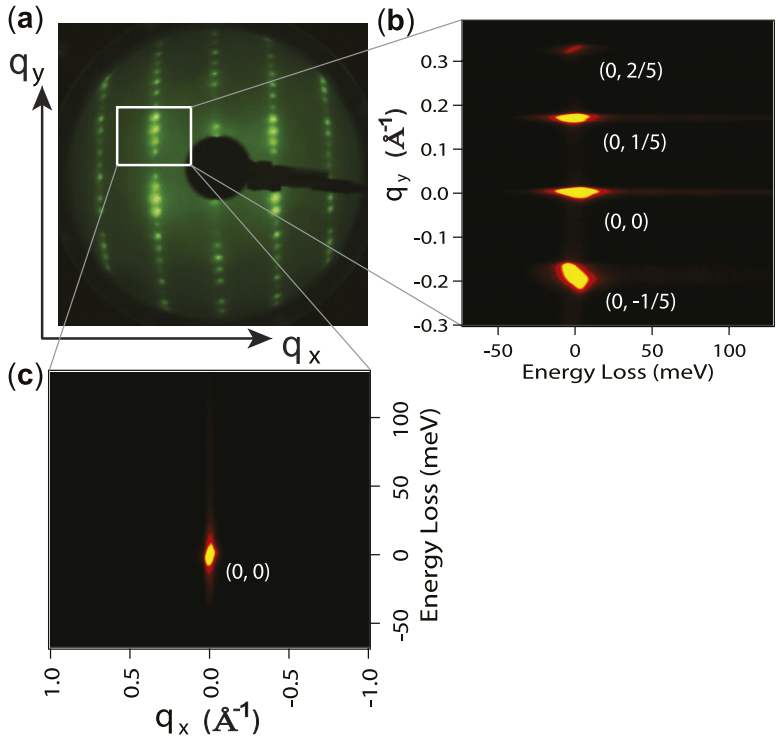

FIG. 6. Elastic peaks from 2D HREELS measurement of Bi2212 at room temperature. (a) LEED pattern of the sample with incident electron energy of 70 eV. There is a 5× reconstruction along the y direction. (b) Elastic peaks of the 2D HREELS along the y direction. (c) Elastic peaks of the 2D HREELS along the x direction.

and direction in the reciprocal space during the HREELS measurement.

In Figs. 6(b) and 6(c), the intensity of the elastic peaks is so strong that the inelastic signals are almost invisible. To see the inelastic signal, one usually needs to move the elastic peaks out of the scanning energy range and then scan the proper energy range for a longer time. For example, instead of the energy range −60 to 120 meV in Fig. 6(c), one can use 50–100 meV to probe the inelastic signals from the phonon branch near 80 meV, as demonstrated in Fig. 7(a). The x direction in Fig. 6 corresponds to the $\Gamma(0,0) - Y(\pi,\pi)$ nodal direction in the BZ of Bi2212, so Fig. 7(a) shows the phonon spectrum

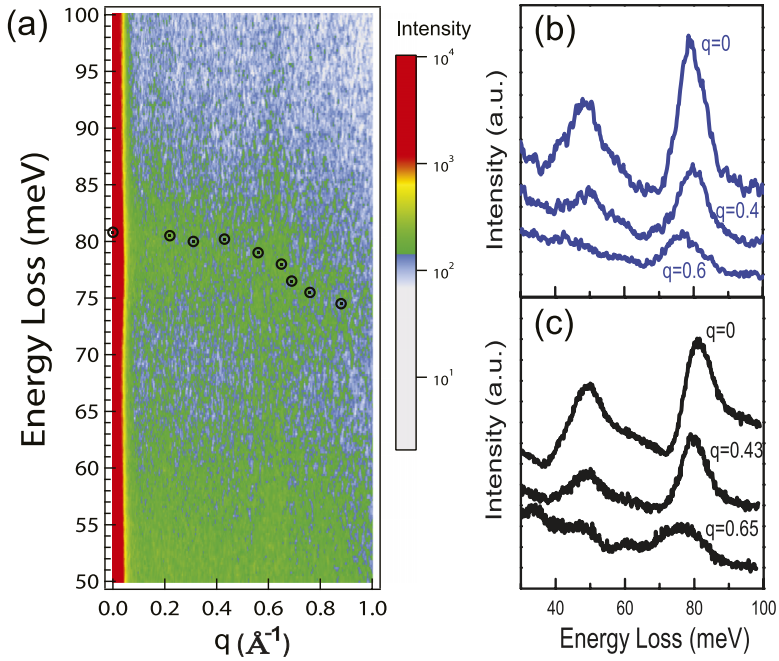

FIG. 7. (a) 2D HREELS energy-momentum mapping of Bi2212 at room temperature, with zoom-in of Fig. 6(c) from 50 to 100 meV energy loss range, showing the inelastic scattering signal from Bi2212 along the nodal direction. The intensity is plotted in logarithmical scale. The dispersion band of the A1g apical oxygen phonon mode is clearly seen. The circles represent the points obtained by conventional HREELS measurements from Ref. 33. (b) The EDC of three different momenta extracted from the 2D mapping. (c) Three 1D spectra for similar momenta by conventional HREELS measurements from Ref. 33.

of Bi2212 along the nodal direction. The phonon branch near 80 meV, corresponding to the A_{1g} apical oxygen mode, shows a clear energy softening when q increases, consistent with the reported results measured by conventional HREELS.[33] With our new system, instead of several discrete energy-momentum points in conventional HREELS measurements, we now have a continuous phonon band.

One of the main advantages of our new HREELS system is that a 2D image like Fig. 7(b) can be scanned in one measurement without rotating sample, monochromator, or analyzer. Due to the large angular mode of the Scienta R4000 hemispherical analyzer, it is now feasible to measure the large momentum values and reach the BZ boundary in one scan. Thus, the measurement efficiency can be greatly improved. For example, in Fig. 7, the 2D spectrum covers the momentum range from 0 to 1 Å $^{-1}$, which reaches the first BZ boundary of Bi2212 in the nodal direction (from 0 to 0.82 Å^{-1}). The sampling time is only limited by the largest momentum point with the smallest signal (about 5 h in our measurement). Based on the data in Fig. 7(a), the 2D image can be used to plot the scattering intensity as a function of energy loss for a given momentum value, which is called the energy distribution curve (EDC). Fig. 7(b) shows the EDCs for three different momentum values. Three 1D EDCs for similar momenta from the conventional HREELS measurements[33] are plotted in Fig. 7(c). The time to accumulate data for the largest momentum transfer is approximately the same in both the new and conventional HREELS systems. But with the 2D detector, all of the momentum EDCs are collected with one scan.

IV. SUMMARY

By integrating the newly designed collimation lens system in the Ibach-type double cylindrical monochromator, we are now able to use a hemispherical electron energy analyzer with 2D detector to perform the HREELS measurements, simultaneously measuring energy and momentum of the inelastically scattered electrons. It is possible with the new HREELS system to measure the dispersion of the phonon modes from the BZ center to the BZ boundary in one scan using the large angular mode of the hemispherical analyzer. The high-momentum-resolution lens produces a very small angular resolution of 0.1°, an order of magnitude improvement.

There are several additional refinements that would increase the capabilities of this instrument. First, we need to explore positioning the sample so that the scattering plane is out of the mirror plane to observe modes forbidden by symmetry in the geometry of the conventional HREELS spectrometer.[36] Second, as Fig. 7 illustrates the background in a HREELS spectrum is large and depends seriously on energy and momentum due to the presence of the elastically scattered beam and the correspondingly excited continuous electron-hole pair excitations. A physics-based model for the background will be developed so that visual displays of the energy-momentum curves without background can be routinely displayed.

ACKNOWLEDGMENTS

We would like to thank Professor Larry Kesmodel for useful discussions for building the electron source. We would also like to thank Professor Genda Gu for providing the Bi2212 samples. This project was funded by NSFC (Nos. 11225422 and 11304367), MOSTC (No. 2012CB921700), and the External Cooperation Program of BIC, CAS (No. 112111KYSB20130007).

[1]H. Ibach and D. L. Mills, *Electron Energy Loss Spectroscopy and Surface Vibrations* (Academic Press, New York, 1982).
[2]P. Brüesch, in *Phonons: Theory and Experiments II*, Springer Series in Solid-State Sciences Vol. 65 (Springer-Verlag, 1986).
[3]W. Kress and F. W. de Wette, *Surface Phonons* (Springer-Verlag, 1991).
[4]M. Rocca, Surf. Sci. Rep. **22**, 1 (1995).
[5]N. Martensson, P. Baltzer, P. Bruhwiler, J.-O. Forsell, A. Nilsson, A. Stenborg, and B. Wannberg, J. Electron Spectrosc. Relat. Phenom. **70**, 117 (1994).
[6]T. Valla, A. V. Fedorov, P. D. Johnson, and S. L. Hulbert, Phys. Rev. Lett. **83**, 2085 (1999).
[7]T. Valla, A. V. Fedorov, P. D. Johnson, B. O. Wells, S. L. Hulbert, Q. Li, G. D. Gu, and N. Koshizuka, Science **285**, 2110 (1999).
[8]A. Damascelli, Z. Hussain, and Z.-X. Shen, Rev. Mod. Phys. **75**, 473 (2003).
[9]C. Fadley, J. Electron Spectrosc. Relat. Phenom. **178-179**, 2 (2010).
[10]R. Comin and A. Damascelli, in *Strongly Correlated Systems*, Springer Series in Solid-State Sciences Vol. 180, edited by A. Avella and F. Mancini (Springer Berlin Heidelberg, 2015), pp. 31–71.
[11]P. Marmet and L. Kerwin, Can. J. Phys. **38**, 787 (1960).
[12]A. L. Hughes and J. H. McMillen, Phys. Rev. **34**, 291 (1929).
[13]G. J. Schulz, Phys. Rev. Lett. **10**, 104 (1963).
[14]C. E. Kuyatt, J. A. Simpson, and S. R. Mielczarek, Phys. Rev. **138**, A385 (1965).
[15]H. Ehrhardt, L. Langhans, F. Linder, and H. S. Taylor, Phys. Rev. **173**, 222 (1968).
[16]H. Ibach, Phys. Rev. Lett. **24**, 1416 (1970).
[17]F. H. Read, J. Phys. E: Sci. Instrum. **3**, 127 (1970).
[18]D. Roy, A. Delage, and J.-D. Carette, J. Phys. E: Sci. Instrum. **8**, 109 (1975).
[19]H. Ibach, J. Electron Spectrosc. Relat. Phenom. **64-65**, 819 (1993).
[20]B. A. Gurney, W. Ho, L. J. Richter, and J. S. Villarrubia, Rev. Sci. Instrum. **59**, 22 (1988).
[21]W. D. Mieher, L. J. Whitman, and W. Ho, J. Chem. Phys. **91**, 3228 (1989).
[22]L. Vattuone and M. Rocca, Rev. Sci. Instrum. **73**, 3861 (2002).
[23]H. Ibach, D. Bruchmann, R. Vollmer, M. Etzkorn, P. S. Anil Kumar, and J. Kirschner, Rev. Sci. Instrum. **74**, 4089 (2003).
[24]R. Vollmer, M. Etzkorn, P. S. A. Kumar, H. Ibach, and J. Kirschner, Phys. Rev. Lett. **91**, 147201 (2003).
[25]G. Ertl and J. Küppers, *Low Energy Electrons and Surface Chemistry* (VCH Verlagsgellschaft, 1985).
[26]T. Nagao and S. Hasegawa, Surf. Interface Anal. **30**, 488 (2000).
[27]H. Claus, A. Büssenschütt, and M. Henzler, Rev. Sci. Instrum. **63**, 2195 (1992).
[28]T. Krebs, G. Andersson, and H. Morgner, Chem. Phys. **340**, 181 (2007).
[29]J. A. Simpson, Rev. Sci. Instrum. **35**, 1698 (1964).
[30]C. E. Kuyatt and J. A. Simpson, Rev. Sci. Instrum. **38**, 103 (1967).
[31]I. E. McCarthy and E. Weigold, Rep. Prog. Phys. **54**, 789 (1991).
[32]H. Ibach, *Electron Energy Loss Spectrometers—The Technology of High Performance* (Springer-Verlag, 1991).
[33]H. Qin, J. Shi, Y. Cao, K. Wu, J. Zhang, E. W. Plummer, J. Wen, Z. Xu, G. Gu, and J. Guo, Phys. Rev. Lett. **105**, 256402 (2010).
[34]Y. Gao, P. Lee, P. Coppens, M. A. Subramania, and A. W. Sleight, Science **241**, 954 (1988).
[35]S. H. Pan, J. O'neal, R. Badzey, C. Chamon, H. Ding, J. Engelbrecht, Z. Wang, H. Eisaki, S. Uchida, A. Gupta *et al.*, Nature **413**, 282 (2001).
[36]J. B. Hannon and E. W. Plummer, J. Electron Spectrosc. Relat. Phenom. **64-65**, 683 (1993).